

Autonomous Image-Plane Robot Control for Martian Lander Operations

E. T. Baumgartner

Dept. of Mechanical Engineering
Michigan Technological University
Houghton, MI 49931

P. S. Schenker

Science and Technology Development Section
Jet Propulsion Laboratory
California Institute of Technology
Pasadena, CA 91109

Abstract

This paper describes the use of an image-plane robot control method known as camera space manipulation for remote planetary surface operations using a three degree-of-freedom arm mounted on a lander base. Because of incompatibilities that may exist in the image-plane target objectives that are required for the camera space manipulation method, the final positioning precision of the arm relative to a point in 3D space is investigated. The experimental system developed required only minimal modifications to the existing Martian lander facility and the system achieved positioning precision on the order of 5 mm or less. Autonomous operation of the system was successfully demonstrated for tasks such as autonomous sample acquisition.

1 Introduction

During future unmanned missions to the surface of the Moon and/or the planets, robotic technology will be utilized to carry out various operational tasks such as digging, sample acquisition or inspection, and construction. Current mission scenarios involve the use of a ground control operator who will communicate with the unmanned lander and will specify certain science objectives to be carried out by the remote robotic devices. Because of the long communication delays that are present during planetary missions, the envisioned robotic systems must operate in an autonomous manner and must be robust in their performance.

This paper documents the development of an experimental robotic system at the Jet Propulsion Laboratory (JPL) which has been designed to demonstrate the capability for autonomous lander operations for future unmanned missions to Mars, specifically the planned Mars Surveyor missions. At JPL, a full scale replica of the Mars lander has been constructed and a new, lightweight, retractable three degree-of-freedom

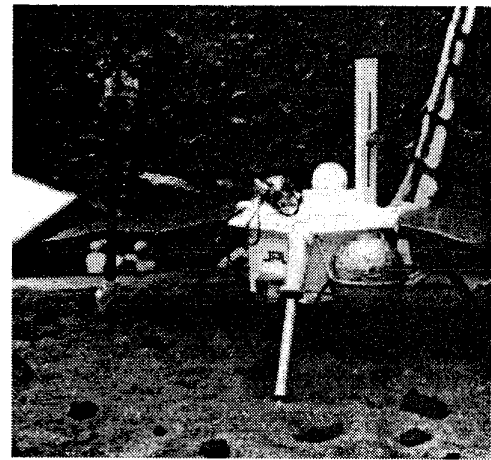


Figure 1: Martian lander robotic facility at JPL.

arm has been fabricated and mounted on the lander base. The entire Martian lander robotic facility is pictured in Figure 1 and the development of this experimental facility is documented in [1]. The tasks addressed by this lander-mounted arm are trenching, sample acquisition and soil inspection. Thus, the point positioning of the robot arm relative to various objects in the near field of the lander base is required of the three degree-of-freedom manipulator.

The control of the robot arm for point positioning tasks is based on the novel method of camera space manipulation [2, 3]. This vision-based method does not rely on any prior knowledge of robot or camera positions (as in calibration-based methods [4]) and the manipulation of the robot is carried out entirely within the reference frame (or image-plane) of the participating cameras without regard to any physical reference frame. Camera space manipulation is a direct method for determining the joint configuration of the robot that achieves the required 3D task objectives and is

distinct from other vision-based methods such as visual servoing [5, 6]. General 3D tasks require a minimum of two typically widely spaced cameras that view a certain region of the manipulator's workspace.

While most applications of camera space manipulation have been focused on terrestrial-based problems, the use of this method for remote, planetary operations has not been studied. Specifically, the target objectives that are identified by a ground control operator in each of the participating camera's image plane may not correspond to a common physical point in 3D space as required by the camera space manipulation method. However, through various experimental studies, small incompatible target objectives were determined not to severely impact the final positioning precision of the developed system.

2 Approach

The method of camera-space manipulation is based on the development of a relationship between the appearance of image-plane features (or "cues") located on a manipulator's end-effector and the manipulator's internal joint configuration. This section outlines how this relationship is developed and implemented for the task of positioning the end-effector of a three degree-of-freedom robot relative to a point in 3D physical space.

2.1 Estimation of View Parameters

Via an orthographic camera model, a point in physical space is projected into the image-plane (or camera-space) of a participating camera by the following relationship [2]:

$$x = (C_1^2 + C_2^2 - C_3^2 - C_4^2)X + 2(C_2C_3 + C_1C_4)Y + 2(C_2C_4 - C_1C_3)Z + C_5 \equiv f_x(X, Y, Z, \mathbf{C}) \quad (1)$$

$$y = 2(C_2C_3 - C_1C_4)X + (C_1^2 - C_2^2 + C_3^2 - C_4^2)Y + 2(C_3C_4 - C_1C_2)Z + C_6 \equiv f_y(X, Y, Z, \mathbf{C}) \quad (2)$$

where a point in physical space is described by the coordinates (X, Y, Z) and the appearance of this point in camera-space is defined by the coordinates (x, y) . The above relationships also contain six view parameters, $\mathbf{C} = [C_1 \ C_2 \ \dots \ C_6]^T$, which are a function of the focal length, and position and orientation of the camera relative to a fixed coordinate frame.

Through the nominal forward kinematics of a robot arm, a physical point on the end-effector of the manipulator is directly related to the internal joint configuration (or joint space) of the manipulator, i.e.

$$\mathbf{R}(\Theta) = [X(\Theta) \ Y(\Theta) \ Z(\Theta)]^T \quad (3)$$

where $\Theta = [\theta_1 \ \theta_2 \ \theta_3]^T$. Therefore, by combining equations (1)–(3), a point in camera-space is directly re-

lated to joint space:

$$x_i^j = f_x(\mathbf{R}_i(\Theta); \mathbf{C}^j) \quad (4)$$

$$y_i^j = f_y(\mathbf{R}_i(\Theta); \mathbf{C}^j) \quad (5)$$

for the i^{th} cue or feature located on the manipulator appearing in the j^{th} camera viewing the robot's workspace.

Thus, by estimating the six view parameters, \mathbf{C}^j , for each participating camera, the relationship between camera-space and joint space is identified. In general, the estimates of the view parameters are computed by minimizing the following least-squared-error performance index:

$$J(\mathbf{C}^j) = \sum_{i=1}^{m_j} \left\{ [x_i^j - f_x(\mathbf{R}_i(\Theta); \mathbf{C}^j)]^2 + [y_i^j - f_y(\mathbf{R}_i(\Theta); \mathbf{C}^j)]^2 \right\} W_i \quad (6)$$

where m_j denotes the total number of measurements (i.e. cues identified) for each camera.

The six view parameters for each participating camera are estimated initially by moving the manipulator through a "preplanned trajectory" which consists of a known set of joint configurations for the manipulator. At each joint configuration, the cue or cues mounted on the manipulator are identified. This large set of simultaneous joint samples and image plane samples of the visual cues provides the initial data set for the determination of the view parameters for each camera. However, by increasing the weighting factor, W_i , in equation (6) as the manipulator moves towards its final objective, the final positioning accuracy is increased by emphasizing those identified cues which are local to the camera-space and joint-space in which the maneuver will terminate.

2.2 Establishing Target Objectives

For the operational task described in this paper, a point on the end-effector of the manipulator is required to be positioned relative to a physical point in 3D space. Therefore, the target objectives for the camera-space manipulation method consist of the image-plane location of a common physical point to be approached by the manipulator in each participating camera. The image-plane location of the common physical target point is denoted by (x_i^j, y_i^j) for each camera and is shown schematically in Figure 2.

For most terrestrial applications, a common target location in each participating camera can be readily identified simply by marking the physical point of interest with a unique feature. However, for planetary

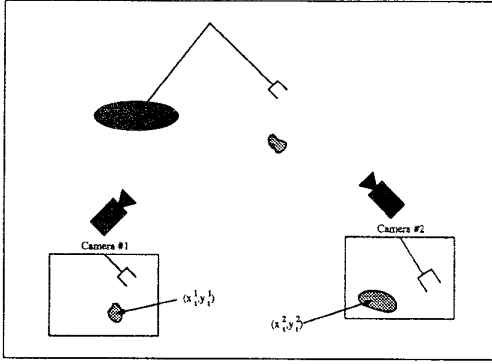


Figure 2: Image-plane target points for sample acquisition.

robotic applications where, for example, a specific soil or rock sample is to be acquired, a common physical point on the sample of interest may not be easily identified. Thus, inconsistencies in the image-plane target points may impact the final positioning precision of the method.

During the experimental trials of the lander-based robotic arm, the target objectives for the system were designated by a ground control station operator. For one of the participating cameras, the operator identified a target point on the sample of interest by positioning a cursor (which was overlaid onto the video image) at a specific location in the image. Then, for each additional camera, the operator again used the cursor to identify what was judged to be an image-plane location which corresponded to the same physical point that was identified in the first camera's image plane. As expected, incompatibilities in the target objectives are present via this approach, however, as will be later discussed, these small target objective incompatibilities did not severely effect the final positioning precision of the method.

2.3 Achieving Target Objectives

With the image-plane target objectives, (x_t^j, y_t^j) , specified as described in the previous subsection and with the view parameters, \mathbf{C}^j , established, the joint configuration, Θ , which positions a desired target location on the end-effector of the manipulator relative to the physical target point in 3D space is found by minimizing the following index:

$$\gamma(\Theta) = \sum_{j=1}^{n_{cam}} \left\{ [x_t^j - f_x(\mathbf{R}_T(\Theta); \mathbf{C}^j)]^2 + [y_t^j - f_y(\mathbf{R}_T(\Theta); \mathbf{C}^j)]^2 \right\} \quad (7)$$

where the desired target location on the manipulator's end-effector is denoted by $\mathbf{R}_T(\Theta)$. The number of cameras that participate in the vision-based guidance of the robot is given by n_{cam} in equation (7). Note that for general 3D tasks, a minimum of two cameras must participate in order to resolve the three joint rotations that position the end-effector relative to the 3D physical target point. Also note that the location of the point on the manipulator to be positioned, $\mathbf{R}_T(\Theta)$, can be arbitrarily specified and will be known through the nominal forward kinematics of the robot.

Therefore, the procedure used to carry out 3D point positioning using camera space manipulation is as follows:

1. Complete the preplanned trajectory and estimate \mathbf{C}^j for the j^{th} participating camera through the minimization of the performance index in equation (6).
2. Identify the target objectives in each participating camera, (x_t^j, y_t^j) . These target objectives describe the possibly incompatible image plane locations of a physical point in 3D space that the manipulator is to approach.
3. Compute intermediate image plane target positions between the current location of the robot's end-effector in the image plane and the overall target objectives in each camera.
4. Determine the joint configuration, Θ , that brings the target location on the manipulator, \mathbf{R}_T , to these intermediate target positions by minimizing the index in equation (7).
5. As the target point on the end-effector of the manipulator moves towards the overall target objective, additional samples of the cue or cues on the manipulator are acquired and the view parameters, \mathbf{C}^j , are re-estimated.
6. Steps 3-5 are repeated until the overall target objectives have been achieved and the target point on the manipulator has approached the target point in 3D space.

Steps 3-6 above indicate that the image-plane target is not approached directly, but instead is approached through a series of intermediate steps. The determination of Θ in Step 4 is aided by this approach by guaranteeing a well-behaved minimization of equation (7). Also, during the re-estimation of the view parameters (Step 5), the weighting factor, W_i , in equation (6) is increased as the manipulator approaches the final target objective, thereby localizing the relationship between joint space and camera space in which

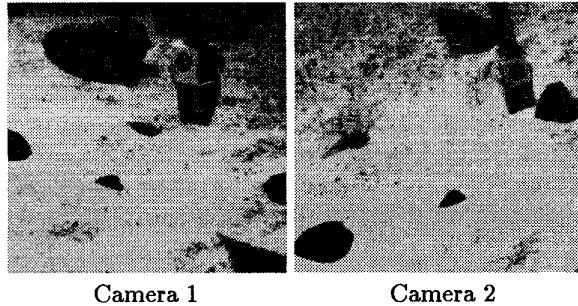


Figure 3: Visual cue mounted on robot end-effector as viewed from lander-mounted cameras.

the maneuver will terminate. This localization of the relationship described by equations (4) and (5) allows the camera space manipulation method to be robust to measurement or modelling errors such as errors in the forward kinematic model of the manipulator.

3 Experimental Facility

The experimental trials conducted to test the method described in this paper were carried out within the laboratory facilities at JPL. A full-scale laboratory replica of a Martian lander envisioned for use in the upcoming NASA Mars Surveyor '98 mission has been constructed and an innovative, lightweight, telescoping three degree-of-freedom arm has been mounted on the lander base as shown previously in Figure 1.

In addition to the lander-based robot arm, two low-cost CCD cameras were mounted on the lander so that the cameras were as widely spaced as possible, and so that both cameras roughly viewed the same region of the manipulator's workspace. Thus, one camera (Camera 1) was mounted below one of the lander's solar panels while one camera (Camera 2) was mounted on a boom approximately 1 meter above the top of the lander base. Acquisition and processing hardware included a 80386-based personal computer and a video framegrabber. Communication with the manipulator (i.e. joint level commands) was carried out via a serial link with the existing low-level robot controller. All experiments were conducted in real-time.

As stated in Section 2.1, a feature or cue on the manipulator must be readily identified to provide the basis for establishing the estimates of the view parameters, C^j , for each camera. For the experimental system described in this paper, a single ring-shaped cue was mounted on the end-effector of the lander's robot arm. This visual cue as viewed by each participating camera is shown in Figure 3 and is rapidly detected via a simple image analysis technique [7]. During previous experimental trials using camera-space manipu-

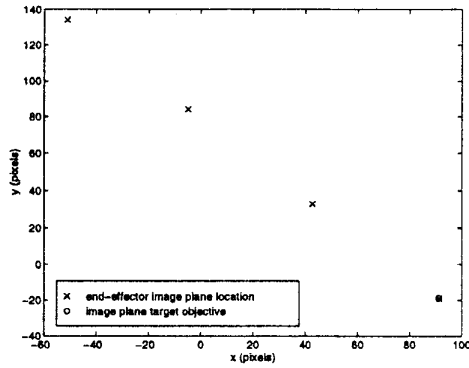
lation, multiple cues have been attached to a robot's end-effector [3]. However, in order to minimize the modifications of the lander-based robot arm, only a single cue was added to the system. While a single cue does reduce the number of measurements available to estimate the view parameters, the use of a single cue did not adversely effect the final positioning precision achieved by the vision-based system as will be shown in the following section.

4 Results

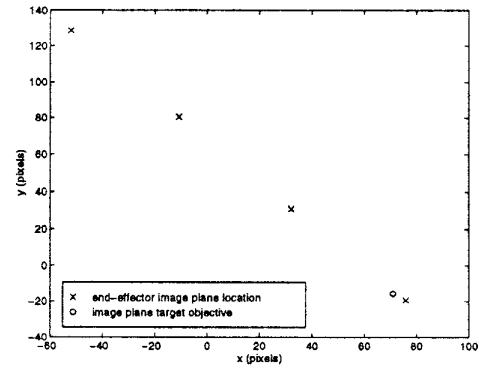
As stated in Section 2.1, the view parameters, C^j , are initially estimated for each camera through the preplanned trajectory. For the experimental trials presented in this paper, the preplanned trajectory consisted of a set of 15 joint configurations. This set of joint configurations were chosen so that the cue mounted on the robot's end-effector spanned a large region of each camera's image plane, thereby assuring that the minimization of equation (6) converged to the correct set of view parameters. It is important to note that while the orthographic projection model given by equations (1) and (2) provides the basis for the estimation process, this model is only an approximation to the superior perspective projection model. However, an approach known as "flattening" [8] was utilized during these experimental trials. This approach allows for the continued use of the orthographic model while incorporating the perspective effect through an iterative methodology which modifies the raw image-plane data to make them consistent with the numerically advantageous orthographic model.

To assess the positioning accuracy of the developed system, the ideal case where a common physical point in 3D space was correctly identified in each of the two participating cameras was considered. This case corresponds to the situation where the target objectives for each camera are compatible with one another. As outlined in Section 2.3, the method of camera space manipulation was used to approach the physical target point through a series of intermediate stages. This approach trajectory as well as each camera's target objective are shown in Figure 4 for Cameras 1 and 2. These figures show that the image plane target objectives are being achieved by the method presented in this paper. The final positioning precision was physically measured by comparing the final position of the target point on the manipulator's end-effector relative to the target location in 3D space. During the trial described above as well as additional trials, the final positioning precision was measured to be 5 mm or less in each of the three physical space directions.

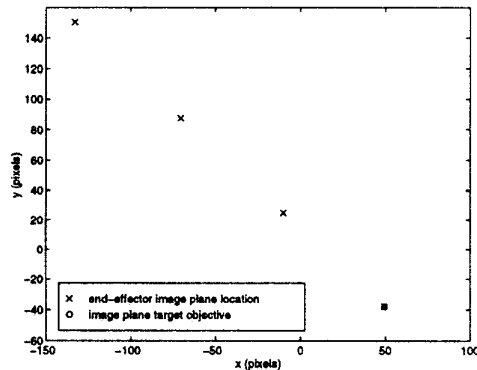
As stated previously, for remote planetary opera-



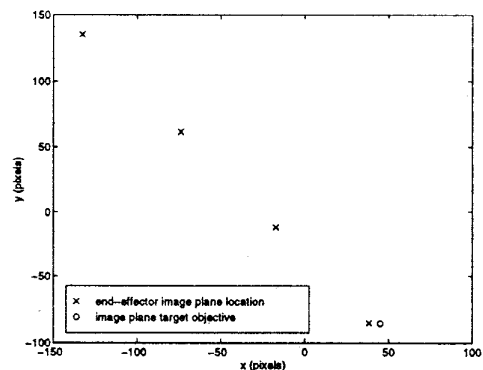
(a)



(b)



(b)



(b)

Figure 4: Image plane approach traj. for compatible target objectives - (a) Camera 1, (b) Camera 2.

Figure 5: Image plane approach traj. for incompatible target objectives - (a) Camera 1, (b) Camera 2.

tions, compatible target objectives will, in general, not be available. Therefore, some incompatibility will exist between the target objective identified in one camera's image plane with respect to the target objective identified in the second camera's image plane. To investigate the effect of incompatible target objectives, an experiment was constructed such that two target points were separated by a distance of 5 cm. Then, one target point was identified in the image plane of Camera 1 and the other target point was identified in the image plane of Camera 2. Thus, the target objectives for each camera did not correspond to a common physical point. The approach of the target point on the manipulator's end-effector to the image-plane target objective for this case is shown in Figure 5 for Cameras 1 and 2, respectively. Note that the target objectives are not being accurately achieved, however, the final joint configuration as calculated by equation (7) attempts to achieve the incompatible target objectives in a least-squared-error sense. Therefore, in the physical space, the target point on the end-effector

does not approach either target objective, but instead approaches a point which is between both physical target points. Future research efforts will focus on the development of a sensitivity analysis to determine the effect of incompatible target objectives on the final positioning precision of the camera space manipulation method.

The final series of experiments conducted were related to the autonomous acquisition of a sample from a soil surface using a powered scoop located on the lander-mounted manipulator. During these experiments, a small rock that was within the workspace of the robot arm and that was within the field of view of the two cameras attached to the lander was identified. The target objectives were specified via a remote operator through the placement of a cursor on the image-plane appearance of the rock for each camera. Since a common physical point was difficult to identify on the sample of interest, as expected, incompatibilities in the target objectives did exist. The target location on the manipulator, \mathbf{R}_T , was chosen such that the powered

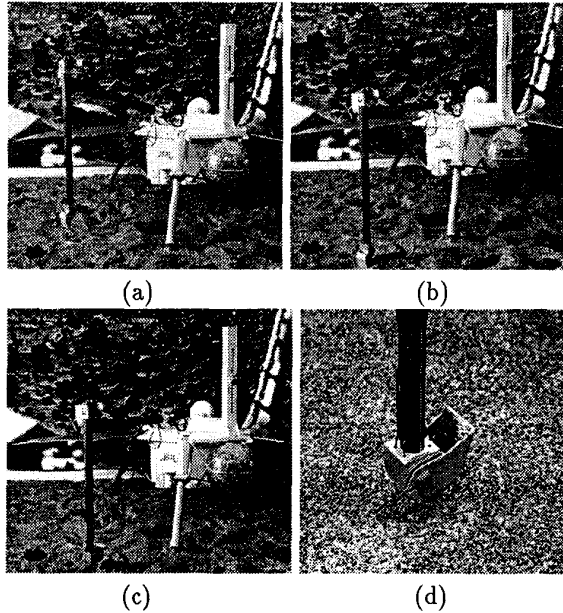


Figure 6: Autonomous acquisition of a soil sample.

scoop was positioned directly over the sample at the end of the approach trajectory. Once positioned over the sample, the powered scoop was actuated to acquire the rock sample. This sequence of events is shown in Figure 6 (a)-(d). Since the sample to be acquired was generally a small object, the resulting incompatibilities in the target objectives did not severely effect the final positioning precision of the method and the sample was accurately and reliably acquired.

5 Conclusions

This paper has presented the development of a image-plane control method for guiding a Martian lander-mounted robot arm for use in remote surface operations. The system required only minor modifications to the current Martian lander replica at JPL. The modifications included the placement of one small cue on the manipulator's end-effector and the mounting of two small CCD cameras on the lander base.

The experimental trials conducted revealed that final positioning precision on the order of 5 mm or less can be expected. This level of positioning precision allowed for the successful autonomous acquisition via a powered scoop of small samples that were found in the near field of the lander. Due to the inherent characteristics of the camera space manipulation method (e.g. knowledge of physical location of cameras and robot is not required), the system developed was viewed as a viable solution to the autonomous op-

eration of remote robotic systems.

Acknowledgments

The authors would like to acknowledge the contributions of Dr. Eric Paljug for the development of the joint-level controller for the lander-mounted arm. The authors would also like to thank Dr. Emilio Gonzalez-Galvan for his software development activities. This project is supported by the NASA Telerobotics and Mars Exploration Technology Program and the 1995 NASA/ASEE Summer Faculty Fellowship Program.

References

- [1] P.S. Schenker, et al., "Mars lander robotics and machine vision capabilities for *in situ* planetary science," *Proceedings of SPIE 2588: Intelligent Robots and Computer Vision XIV*, Philadelphia, PA, October, 1995.
- [2] S.B. Skaar, W.H. Brockman, and W.S. Jang, "Three dimensional camera-space manipulation," *Int. J. of Robotics Research*, Vol. 9, No. 4, pp. 22-39, 1991.
- [3] S.B. Skaar and E. Gonzalez-Galvan, "Versatile and precise vision-based manipulation," in *Teleoperation and Robotics in Space*, S.B. Skaar and C.F. Ruoff, eds., Chapter 9, AIAA Press, Washington, September, 1994.
- [4] R.Y. Tsai, "A versatile camera calibration technique for high-accuracy 3D machine vision metrology using off-the-shelf TV cameras and lenses," *IEEE Trans. on Robotics and Automation*, Vol. 3, No. 4, pp. 323-344, 1987.
- [5] L.E. Weiss, A.C. Sanderson, C.P. Neuman, "Dynamic sensor-based control of robots with visual feedback," *IEEE Trans. on Robotics and Automation*, Vol. 3, No. 5, pp. 404-471, 1987.
- [6] B. Espiau, F. Chaumette, P. Rives, "A new approach to visual servoing in robots," *IEEE Trans. on Robotics and Automation*, Vol. 8, No. 3, pp. 313-326, 1992.
- [7] S.B. Skaar, W.Z. Chen, and R.K. Miller, "High resolution camera-space manipulation," *Proc. ASME Design Automation Conf.*, Miami, FL, Sept., 1991.
- [8] E. Gonzalez-Galvan, S.B. Skaar, U. Korde, and W.Z. Chen, "A precision-enhancing measure in 3-D rigid-body positioning using camera-space manipulation," to appear in the *International Journal of Robotics Research*.